Distribution of solute atoms in β- and spinel $Si_{6-z}Al_zO_zN_{8-z}$ by Al *K*-edge x-ray absorption near-edge structure

Kazuyoshi Tatsumi,[1] Teruyasu Mizoguchi,[2] Satoru Yoshioka,[3] Tomoyuki Yamamoto,[4] Takeo Suga,[4] Toshimori Sekine,[5] and Isao Tanaka[3]

[1]*Department of Materials, Physics and Energy Engineering, Nagoya University, Chikusa, Nagoya 464-8603, Japan*

[2]*Institute of Engineering Innovation, The University of Tokyo, Bunkyo, Tokyo 113-8656, Japan*

[3]*Department of Materials Science and Engineering, Kyoto University, Sakyo, Kyoto 606-8501, Japan*

[4]*Fukui Institute for Fundamental Chemistry, Kyoto University, Sakyo, Kyoto 606-8103, Japan*

[5]*Advanced Materials Laboratory, National Institute for Materials Science, Namiki, Tsukuba 305-0044, Japan*

(Received 20 July 2004; published 27 January 2005)

Local environments of solutes in β- and spinel $Si_{6-z}Al_zO_zN_{8-z}$ are investigated by means of Al *K* x-ray absorption near-edge structure. The experimental spectra are found to be the same throughout the wide solubility range. This suggests that the local environments of Al are independent of the solute concentration. First-principles band-structure calculations are systematically made to interpret the experimental spectra. Effect of a core hole was included into the calculation. Theoretical spectra were obtained using variety of different model structures constructed by a set of plane-wave pseudopotentials calculations in our previous study [K. Tatsumi, I. Tanaka, H. Adachi, and M. Yoshiya, Phys. Rev. B **66**, 165210 (2002)]. The numbers of models were 51 and 45 for both β and spinel, respectively. They are classified and averaged according to the local atomic structure of Al solutes. The combination of experimental spectra and theoretical results can unambiguously lead to the conclusion that Al atoms are preferentially coordinated by O atoms in both β and spinel phases. This is consistent with the conclusion obtained by the first-principles total-energy calculations. In the spinel phase, Al atoms are found to be located preferentially at the octahedral cationic site. This agrees with the conclusion in a recent report on the nuclear magnetic resonance experiment.

DOI: 10.1103/PhysRevB.71.033202 PACS number(s): 71.20.Nr, 61.66.Dk, 61.10.Ht, 78.40.Pg

Silicon nitride–based ceramics have been widely studied as high-temperature structural materials and gate dielectrics in microelectronic applications.[1,2] The solid solutions of Si_3N_4 with Al and O are denoted SiAlONs, of which the chemical formula is often given by $Si_{6-z}Al_zO_zN_{8-z}$.[3,4] Their material properties are known to deviate from those of Si_3N_4 by the solution depending upon the content of the solutes, i.e., the *z* number.[5,6] Dense β-SiAlONs were successfully synthesized without sintering additives using the hot isostatic pressing method, and their physical properties were investigated.[7] Their mechanical properties such as elastic moduli were found to decrease linearly with increasing *z*. The lattice softening caused by the solutes is essentially important for their mechanical performance, enabling different kinds of applications. The solution effects should be strongly related to the distribution of the solute atoms. However, only little is known about the distribution. As a new member of the SiAlON family, a cubic spinel phase was recently synthesized by high-pressure experiments.[8,9] Distribution of solutes in the spinel SiAlON is interesting as well as that of ordinary hexagonal phases.

We have recently examined first principles energetics of substitutional solutes in β- and spinel SiAlONs using a plane-wave pseudopotential calculation.[10] We found that Al and O prefer to be bound at the nearest-neighbor sites when they are dissolved in Si_3N_4. The pairing of Al and O atoms has a benefit in energy by a few tenths of eV per an Al-O pair. The theoretical result is consistent with previous experimental studies using ^{27}Al and ^{29}Si magic-angle-spinning nuclear magnetic resonance (MAS-NMR).[11–13] These studies concluded that Al-O and Si-N bonds are predominant. Several theoretical works showed a similar tendency of the solutes in SiAlONs.[14–17] Our calculations also suggested that physical properties such as the band gap can only be explained when such pairing is fully taken into account. Sekine *et al.* reported ^{29}Si MAS-NMR from the spinel phase, which implies a similar bond preference.[8]

In this study, we aim to give a detailed analysis on the local structures of the solutes in β- and spinel SiAlONs using Al *K* x-ray absorption near-edge structure (XANES). First principles calculations are systematically made to interpret the spectra. Al *K* XANES can reveal the chemical environments around the solute Al atoms, because it reflects local and partial density of states for unoccupied *p*-like states around excited Al atoms. To the authors' best knowledge, there have been no reports on XANES of the SiAlON phases.

The maximum solubility of β-SiAlON was reported to be $z=3.8$[5]. β-SiAlON samples were prepared at $z=0.23$, 0.50, 2.0, and 3.0. They were chosen to represent both dilute and high concentration solid solutions. The samples of $z=0.23$ and 0.50 were prepared by sintering of the mixture of commercial ceramic powders of Si_3N_4, AlN, and Al_2O_3 in N_2 gas with the pressure of 0.925 MPa and 1900 °C for 1 h. The high pressure of N_2 is necessary to minimize the decomposition of Si_3N_4. Samples with $z=2.0$ and 3.0 were prepared by hot isostatic pressing of glass encapsulated samples at 170 MPa and 1800 °C for 2 *h*.[7] Powder x-ray diffraction study found that the only crystalline phase in these samples was β-SiAlON. It is known that the surface of silicon nitride powder is easily oxidized. In our experience, however, the surficial silicon oxides can be easily distinguished from that

of SiAlON by the Si *K* XANES when SiAlONs are oxidized at high temperatures. The present SiAlONs samples did not show any peaks of the silicon oxides, confirming the absence of detectable amount of surface oxides. Cubic-spinel-type SiAlONs were synthesized by the shock compression technique.[8] The samples are identical to those of Ref. 8. Compositions of the samples were $z=1.8$ and 2.3.

Al *K* XANES are collected in a total electron yield mode at room temperature using a $KTiOPO_4$ (KTP) two-crystal monochrometer at the BL1A of the UVSOR, Institute for Molecular Science, Okazaki, Japan. The energy width of the monochromatized beam is 0.5–0.6 eV.[18] Commercial powders of wurzite-AlN (*w*-AlN) and corundum-Al_2O_3 (*cr*-Al_2O_3) were also measured as references. All samples are well ground and mounted on adhesive carbon tapes in order to avoid surface charging.

In order to interpret the experimental Al *K* XANES from SiAlONs, theoretical calculations of XANES were made using the *ab initio* orthogonalized linear combination of atomic orbitals (OLCAO) method[19] with local approximation to the density functional theory. The method has been confirmed to reproduce the experimental XANES satisfactorily in a number of wide-gap compounds.[20–26] A rigorous scheme to include the core-hole effect as implemented in the OLCAO method is mandatory for such quantitative reproduction of the experimental spectra.[20] In the present calculations, 42-atom and 56-atom supercells for β- and spinel SiAlONs were adopted. These supercells correspond to a $1\times1\times3$ array of unit cell of β and a conventional unit cell of spinel, respectively. The atomic structure is optimized within the unit cell in our previous calculations.[10] This structure is expanded to be a supercell. It is confirmed that the main peak positions in theoretical XANES are not altered when larger supercells.

The theoretical intensity of XANES is obtained from the calculation of the dipole transition matrix between ground and final states. 8 **k** points in the whole Brillouin zone of the supercell were used in the spectral calculation. The final spectrum was broadened by a Gaussian function with a full width at half maximum (FWHM) of 1.0 eV. We do not prefer to use the broadening factor as means to improve the agreement with the experimental spectra. Real solutes are in various atomic arrangements, which make apparent peak broadening in the experimental spectra. This cannot be computed completely within the number of our calculated models. The transition energy of the theoretical spectrum was obtained from the difference of the electronic total energies of the supercell at the final and ground states.

Figure 1 shows the experimental Al *K* XANES from β-SiAlONs and two reference compounds. Two points are noteworthy in Fig. 1. First, the spectral shapes of β-SiAlONs are almost the same for all the compositions. This suggests that local environments of Al are similar from $z=0.23$ to 3.0. Second, clear chemical shifts among *w*-AlN, *cr*-Al_2O_3, and β-SiAlONs can be found. The first peaks of SiAlONs are located at the middle of those of *w*-AlN and *cr*-Al_2O_3. It is higher by 1.7 eV than that of *w*-AlN and 2.4 eV lower than that of *cr*-Al_2O_3. In order to investigate these features, we obtained theoretical spectra by a first-principles method.

Before examining the theoretical results of SiAlONs, we have examined how well the reproduction of experimental

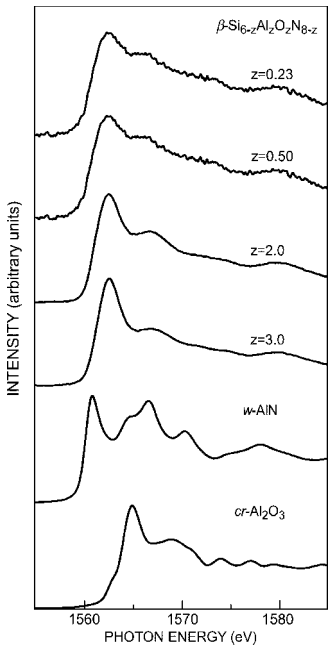

FIG. 1. Experimental Al *K* XANES from β-SiAlONs (with $z=0.23$, 0.50, 2.0, and 3.0) and two reference compounds, *w*-AlN and *cr*-Al_2O_3.

spectrum can be made. Figure 2 shows the results for two reference compounds, *w*-AlN and *cr*-Al_2O_3. The theoretical results reproduce the spectral shapes well. The experimental chemical shift of the first peaks as denoted by short solid lines is 4.1 eV. The theoretical spectra show reproduction of the energy shift within an accuracy of <0.1 eV. Since the theoretical calculation can reproduce the experimental chemical shifts with such accuracy, the experimental peak position of the SiAlON spectra can be quantitatively compared to the theoretical peak positions. The comparison should lead to real local environments of the solute Al.

In Fig. 3, we compare the theoretical spectra of β-SiAlONs with the experimental ones. In our previous study, we have examined all possible solute arrangements of SiAlONs within the unit cell composed of 14 atoms. They were altogether 29 different kinds of cells for six solute concentrations ($z=1,2,\ldots,6$). In the present study, two new cells at $z=6$ were added to the previous 29 cells. Among $29+2=31$ cells, we have chosen three cells with first, second and third lowest formation energies at each z for the Al *K* XANES calculations. The number of cells examined was $3\times6=18$. Since some of structures include multiple Al sites of different crystallographic symmetry, there were totally 51 different Al sites in the 18 cells. The XANES calculations were made for all of these 51 Al sites using supercells composed of 42 atoms, i.e., $1\times1\times3$ array of the unit cell. The 51 spectra were classified and averaged according to the local coordinations of the excited Al atoms. The number of different spectra were 1, 5, 18, 20, and 7 for AlN_4, $AlON_3$, AlO_2N_2, AlO_3, and AlO_4, respectively. Figure 3 shows five theoretical spectra by averaging them within the same class of AlO_nN_{4-n} ($n=0,1,\ldots,4$). The theoretical transition energy was calibrated in such a way that the first peak of theoretical spectra of *w*-AlN is set at the experimental spectrum

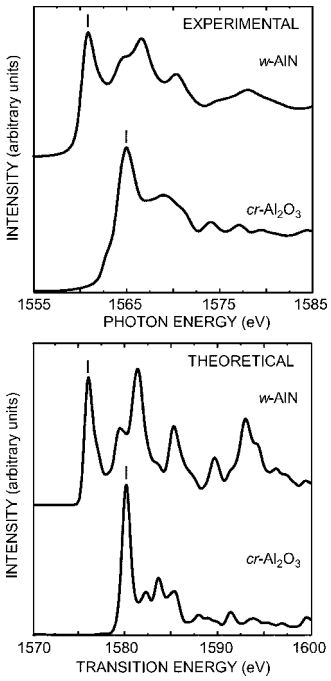

FIG. 2. Theoretical spectra of *w*-AlN and *cr*-Al_2O_3 are compared with the experimental ones. The theoretical transition energy is shifted so that the first peak of the theoretical spectrum for *w*-AlN is aligned with that of the corresponding experimental spectrum.

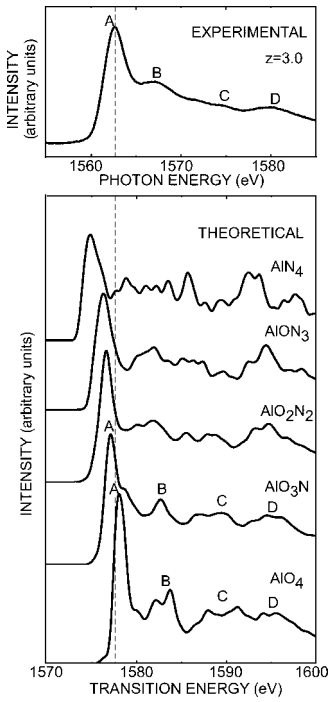

FIG. 3. Comparison of experimental and theoretical Al *K* XANES from β-SiAlONs. The experimental spectra are represented by the case of $z=3.0$. The dashed line shows the energy corresponding to the experimental first peak position. The label for each theoretical spectrum as AlO_nN_{4-n} indicates the local coordination of Al atoms in the 42-atom supercell.

of *w*-AlN. The theoretical first peak moves toward higher energy by 3.3 eV from AlN_4 to AlO_4. Among the collected theoretical spectra, the standard deviation of the first peak positions is <0.4 eV within each group of $AlO_{1-x}N_x$.

The experimental first peak of β-SiAlON is located in between those of the theoretical spectra of AlO_3N and AlO_4. As seen in Fig. 1, this peak position does not change with the solute concentration. These results imply that Al solutes in β-SiAlONs are preferentially coordinated by O solutes independently of the solute concentration. Major local coordinations of the solute Al are therefore interpreted to be AlO_3N and AlO_4. This is consistent with the conclusion of our previous study showing that Al-O and Si-N bonds are clearly preferred in β-SiAlONs.[10] It should also be noted that the theoretical spectra for AlO_3N and AlO_4 can reproduce the experimental spectral shape quite satisfactorily. This confirms the validity of our theoretical models.

The Al *K* XANES of spinel SiAlONs are analyzed in a similar way. The experimental spectra for two spinel samples are shown in the upper panel of Fig. 4. Theoretical spectra are shown in the same figure. As the case of β-SiAlONs, the atomic arrangements on the unit cell composed of 14 atoms were obtained in our previous study.[10] 42 different kinds of cells were examined in that study. Among them, 18 cells with low formation energies were chosen. A spinel-type crystal structure has two kinds of cationic sites. It possesses 8 tetrahedral (*T*) and 16 octahedral (*O*) sites in a conventional unit cell. There were 45 different Al sites in the selected 18 cells. XANES calculations were made for the 45 different sites using supercells composed of 56 atoms. Similar to the case of β-SiAlONs, the theoretical spectra are classified by the local coordination of the excited Al atoms. They are averaged within the same classes. The left panel shows theoretical Al *K* spectra from *O* sites, while the right shows those from *T* sites. The transition energy was calibrated a method identical to that used in Fig. 3.

The major features of the experimental spectra are denoted by labels A, B, and C. Theoretical spectra for both of the sites show chemical shifts toward higher energy with an increase in the number of coordinating oxygen. The first peak of the theoretical spectra of *O* sites as denoted by short solid lines shows chemical shifts by 2.8 eV from AlN_6 to AlO_6. The standard deviation of the peak positions is <0.5 eV among the spectra within each class of $AlO_{1-x}N_x$. The position of peak A agrees better with the results of AlO_6 or AlO_5N. A similar chemical shift can be found in the theoretical spectra of *T* sites. However, the shape of the *O*-site spectra, especially presence of peak B, is in better agreement with the experimental spectra than that of the *T* site.

Looking at the trends in the *O*-site spectra, one can find that the areal ratio of peak A to peak B increases with the increase of the oxygen coordination. The experimental spectra are best reproduced when AlO_6 or AlO_5N are adopted. Not only the first peak position but also the spectral shape strongly implies that Al atoms tend to occupy the *O* sites, and they prefer to be coordinated by O atoms, not by N atoms. The result from XANES is consistent with our previous calculations, as is the case of β-SiAlONs. Sekine *et al.* reported the ^{29}Si MAS-NMR spectra from spinel SiAlONs. They concluded that Al occupies *O* sites and is coordinated by six oxygen atoms.[8] The present XANES results are also consistent with the NMR results. In our previous calcula-

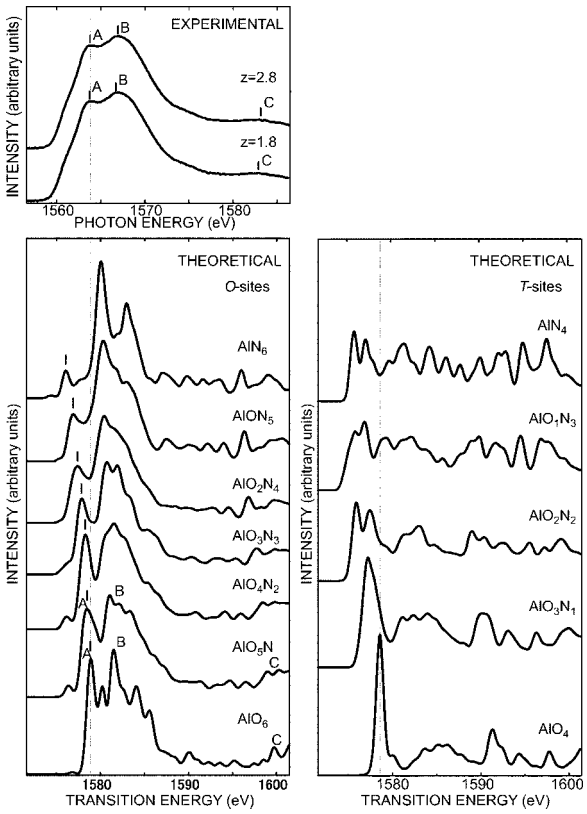

FIG. 4. Comparison of experimental and theoretical Al *K* XANES from spinel SiAlONs. Dashed lines show the position corresponding to peak A of the experimental spectra.

tions, however, the preference of Al at the *O* site as compared to the *T* site was not found. The reason for the discrepancy is still left open. More detailed total-energy calculations using larger supercells to increase the variety of the atomic arrangements may be required. Alternatively, the discrepancy could be ascribed to finite temperature effects, since the calculations were done for ground states.

Finally, major results are summarized as follows:

(1) The shapes of the experimental spectra of β-$Si_{6-z}Al_zO_zN_{8-z}$ were unchanged from $z=0.23-3.0$, which suggests the local environments of Al are independent of the composition.

(2) The present first-principles calculation was found to reproduce not only the spectral shapes but also the chemical shifts of reference materials quantitatively well.

(3) Theoretical XANES spectra for β-SiAlONs were obtained using 51 different model structures constructed by a set of plane-wave pseudopotentials calculations in Ref. 10. They were classified into 5 groups as denoted by AlO_nO_{4-n} $(n=0,1,\ldots,4)$. Theoretical spectra were averaged within the same classes.

(4) The position of the first peak indicated that Al solutes in β-SiAlONs are coordinated preferentially by O solutes, i.e., major local environments are expressed by AlO_3N and AlO_4. Good agreements between the spectral shapes of the theoretical and the experimental spectra can also be found when the results of AlO_3N and AlO_4 were used. This result is consistent with the conclusion of Ref. 10 by theoretical calculations that show a strong preference of Al-O bonds.

(5) Al *K* XANES experiments and theoretical calculations were made also for spinel SiAlONs. 45 different model structures were used. We can conclude that Al solutes are preferentially present at the *O* sites of the spinel structure. Both the magnitude of the chemical shift and the spectral shape imply that the local environment of Al is close to AlO_5N and AlO_6. This result is also consistent with the conclusion of Ref. 10.

This work was supported by the grant-in-aid for scientific research on priority areas (No. 751) and computational materials science program from MEXT of Japan. K.T. and M.T. were supported by JSPS. The authors thank Dr. N. Hirosaki and Dr. Y. Yamamoto for help in sample preparation, Dr. E. Shigemasa, Dr. N. Kondo, Dr. H. Yoshida, and Dr. T. Yoshida for their help in experimental works at UVSOR, and Dr. W.Y. Ching for allowing us to use the OLCAO code.

[1] G. Petzow and M. Herrmann, Structure and Bonding **102**, 47 (2002).
[2] I. V. Belyi, *Silicon Nitride in Electronics* (Elsevier, Amsterdam, 1988).
[3] K. H. Jack and W. I. Wilson, Nature (London), Phys. Sci. **238**, 28 (1972).
[4] Y. Oyama and O. Kamigaito, Jpn. J. Appl. Phys. **10**, 1637 (1971).
[5] T. Ekstrom, J. Am. Ceram. Soc. **75**, 259 (1992).
[6] M. H. Lewis, in *Silicon Nitride Ceramics*, Materials Research Society Symposium Proceedings No. 287, edited by I. W. Chen, P. F. Becher, M. Mitomo, G. Petzow, and T. S. Yen (Materials Research Society, Pittsburgh, 1993), pp. 159–172.
[7] I. Tanaka *et al.*, Acta Metall. Mater. **40**, 1995 (1992).
[8] T. Sekine *et al.*, Chem. Phys. Lett. **344**, 395 (2001).
[9] M. Schwarz *et al.*, Angew. Chem., Int. Ed. **41**, 789 (2002).
[10] K. Tatsumi *et al.*, Phys. Rev. B **66**, 165210 (2002).
[11] N. D. Butler *et al.*, J. Mater. Sci. Lett. **3**, 469 (1984).
[12] R. Dupree *et al.*, J. Mater. Sci. Lett. **4**, 393 (1985).
[13] R. Dupree *et al.*, J. Appl. Crystallogr. **21**, 109 (1988).
[14] S. V. Okatov and A. L. Ivanovskii, Int. J. Inorg. Mater. **3**, 923 (2001).
[15] C. M. Fang and R. Metselaar, J. Am. Ceram. Soc. **86**, 1956 (2003).
[16] C. M. Fang and R. Metselaar, J. Mater. Chem. **13**, 335 (2003).
[17] L. Ouyang and W. Y. Ching, Appl. Phys. Lett. **81**, 8 (2002).
[18] Y. Takata and N. Kosugi, UVSOR Activity Report No. 1999 (2000), p. 112.
[19] W. Y. Ching, J. Am. Ceram. Soc. **73**, 3135 (1990).
[20] S. D. Mo and W. Y. Ching, Phys. Rev. B **62**, 7901 (2000).
[21] S. D. Mo and W. Y. Ching, Appl. Phys. Lett. **78**, 3809 (2001).
[22] W. Y. Ching *et al.*, J. Am. Ceram. Soc. **85**, 11 (2002).
[23] I. Tanaka *et al.*, Appl. Phys. Lett. **78**, 2134 (2001).
[24] T. Mizoguchi *et al.*, Phys. Rev. B **70**, 045103 (2004).
[25] I. Tanaka *et al.*, Nat. Mater. **2**, 541 (2003).
[26] T. Mizoguchi *et al.*, Micron **34**, 249 (2003).